

## THE SLOAN DIGITAL SKY SURVEY: TECHNICAL SUMMARY

DONALD G. YORK,<sup>1</sup> J. ADELMAN,<sup>2</sup> JOHN E. ANDERSON, JR.,<sup>2</sup> SCOTT F. ANDERSON,<sup>3</sup> JAMES ANNIS,<sup>2</sup> NETA A. BAHCALL,<sup>4</sup> J. A. BAKKEN,<sup>2</sup> ROBERT BARKHouser,<sup>5</sup> STEVEN BASTIAN,<sup>2</sup> EILEEN BERMAN,<sup>2</sup> WILLIAM N. BOROSKI,<sup>2</sup> STEVE BRACKER,<sup>2</sup> CHARLIE BRIEGEL,<sup>2</sup> JOHN W. BRIGGS,<sup>6</sup> J. BRINKMANN,<sup>7</sup> ROBERT BRUNNER,<sup>8</sup> SCOTT BURLES,<sup>1</sup> LARRY CAREY,<sup>3</sup> MICHAEL A. CARR,<sup>4</sup> FRANCISCO J. CASTANDER,<sup>1,9</sup> BING CHEN,<sup>5</sup> PATRICK L. COLESTOCK,<sup>2</sup> A. J. CONNOLLY,<sup>10</sup> J. H. CROCKER,<sup>5</sup> ISTVÁN CSABAI,<sup>5,11</sup> PAUL C. CZARAPATA,<sup>2</sup> JOHN ERIC DAVIS,<sup>7</sup> MAMORU DOI,<sup>12</sup> TOM DOMBECKI,<sup>1</sup> DANIEL EISENSTEIN,<sup>1,13,14</sup> NANCY ELLMAN,<sup>15</sup> BRIAN R. ELMS,<sup>4,16</sup> MICHAEL L. EVANS,<sup>3</sup> XIAOHUI FAN,<sup>4</sup> GLENN R. FEDERWITZ,<sup>2</sup> LARRY FISCHELLI,<sup>1</sup> SCOTT FRIEDMAN,<sup>5</sup> JOSHUA A. FRIEMAN,<sup>1,2</sup> MASATAKA FUKUGITA,<sup>13,17</sup> BRUCE GILLESPIE,<sup>7</sup> JAMES E. GUNN,<sup>4</sup> VIJAY K. GURBANI,<sup>2</sup> ERNST DE HAAS,<sup>4</sup> MERLE HALDEMAN,<sup>2</sup> FREDERICK H. HARRIS,<sup>18</sup> J. HAYES,<sup>7</sup> TIMOTHY M. HECKMAN,<sup>5</sup> G. S. HENNESSY,<sup>19</sup> ROBERT B. HINDSLEY,<sup>20</sup> SCOTT HOLM,<sup>2</sup> DONALD J. HOLMGREN,<sup>2</sup> CHI-HAO HUANG,<sup>2</sup> CHARLES HULL,<sup>21</sup> DON HUSBY,<sup>2</sup> SHIN-ICHI ICHIKAWA,<sup>16</sup> TAKASHI ICHIKAWA,<sup>22</sup> ŽELJKO IVEZIĆ,<sup>4</sup> STEPHEN KENT,<sup>2</sup> RITA S. J. KIM,<sup>4</sup> E. KINNEY,<sup>7</sup> MARK KLAENE,<sup>7</sup> A. N. KLEINMAN,<sup>7</sup> S. KLEINMAN,<sup>7</sup> G. R. KNAPP,<sup>4</sup> JOHN KORIENEK,<sup>2</sup> RICHARD G. KRON,<sup>1,2</sup> PETER Z. KUNSZT,<sup>5</sup> D. Q. LAMB,<sup>1</sup> B. LEE,<sup>2</sup> R. FRENCH LEGER,<sup>3</sup> SIRILUK LIMMONGKOL,<sup>3</sup> CARL LINDENMEYER,<sup>2</sup> DANIEL C. LONG,<sup>7</sup> CRAIG LOOMIS,<sup>7</sup> JON LOVEDAY,<sup>1</sup> RICH LUCINIO,<sup>7</sup> ROBERT H. LUPTON,<sup>4</sup> BRYAN MACKINNON,<sup>2,23</sup> EDWARD J. MANNERY,<sup>3</sup> P. M. MANTSCH,<sup>2</sup> BRUCE MARGON,<sup>3</sup> PEREGRINE MCGEHEE,<sup>24</sup> TIMOTHY A. MCKAY,<sup>25</sup> AVERY MEIKSIN,<sup>26</sup> ARONNE MERELLI,<sup>27</sup> DAVID G. MONET,<sup>18</sup> JEFFREY A. MUNN,<sup>18</sup> VIJAY K. NARAYANAN,<sup>4</sup> THOMAS NASH,<sup>2</sup> ERIC NEILSEN,<sup>5</sup> RICH NESWOLD,<sup>2</sup> HEIDI JO NEWBERG,<sup>2,28</sup> R. C. NICHOL,<sup>27</sup> TOM NICINSKI,<sup>2,29</sup> MARIO NONINO,<sup>30</sup> NORIO OKADA,<sup>16</sup> SADANORI OKAMURA,<sup>12</sup> JEREMIAH P. OSTRIKER,<sup>4</sup> RUSSELL OWEN,<sup>3</sup> A. GEORGE PAULS,<sup>4</sup> JOHN PEOPLES,<sup>2</sup> R. L. PETERSON,<sup>2</sup> DONALD PETRAVICK,<sup>2</sup> JEFFREY R. PIER,<sup>18</sup> ADRIAN POPE,<sup>27</sup> RUTH PORDES,<sup>2</sup> ANGELA PROSAPIO,<sup>2</sup> RON RECHENMACHER,<sup>2</sup> THOMAS R. QUINN,<sup>3</sup> GORDON T. RICHARDS,<sup>1</sup> MICHAEL W. RICHMOND,<sup>31</sup> CLAUDIO H. RIVETTA,<sup>2</sup> CONSTANCE M. ROCKOSI,<sup>1</sup> KURT RUTHMANSDORFER,<sup>2</sup> DALE SANDFORD,<sup>6</sup> DAVID J. SCHLEGEL,<sup>4</sup> DONALD P. SCHNEIDER,<sup>32</sup> MAKI SEKIGUCHI,<sup>17</sup> GARY SERGEY,<sup>2</sup> KAZUHIRO SHIMASAKU,<sup>12</sup> WALTER A. SIEGMUND,<sup>3</sup> STEPHEN SMEE,<sup>5</sup> J. ALLYN SMITH,<sup>25</sup> S. SNEDDEN,<sup>7</sup> R. STONE,<sup>18</sup> CHRIS STOUGHTON,<sup>2</sup> MICHAEL A. STRAUSS,<sup>4</sup> CHRISTOPHER STUBBS,<sup>3</sup> MARK SUBBARAO,<sup>1</sup> ALEXANDER S. SZALAY,<sup>5</sup> ISTVÁN SZAPUDI,<sup>33</sup> GYULA P. SZOKOLY,<sup>5</sup> ANIRUDDA R. THAKAR,<sup>5</sup> CHRISTY TREMONTI,<sup>5</sup> DOUGLAS L. TUCKER,<sup>2</sup> ALAN UOMOTO,<sup>5</sup> DAN VANDEN BERK,<sup>2</sup> MICHAEL S. VOGELEY,<sup>34</sup> PATRICK WADDELL,<sup>3</sup> SHU-I WANG,<sup>1</sup> MASARU WATANABE,<sup>35</sup> DAVID H. WEINBERG,<sup>36</sup> BRIAN YANNY,<sup>2</sup> AND NAOKI YASUDA<sup>16</sup>

(THE SDSS COLLABORATION)

Received 2000 February 13; accepted 2000 June 8

## ABSTRACT

The Sloan Digital Sky Survey (SDSS) will provide the data to support detailed investigations of the distribution of luminous and nonluminous matter in the universe: a photometrically and astrometrically calibrated digital imaging survey of  $\pi$  sr above about Galactic latitude  $30^\circ$  in five broad optical bands to a depth of  $g' \sim 23$  mag, and a spectroscopic survey of the approximately  $10^6$  brightest galaxies and  $10^5$  brightest quasars found in the photometric object catalog produced by the imaging survey. This paper summarizes the observational parameters and data products of the SDSS and serves as an introduction to extensive technical on-line documentation.

**Key words:** cosmology: observations — instrumentation: miscellaneous

<sup>1</sup> Department of Astronomy and Astrophysics, University of Chicago, 5640 South Ellis Avenue, Chicago, IL 60637.

<sup>2</sup> Fermi National Accelerator Laboratory, P.O. Box 500, Batavia, IL 60510.

<sup>3</sup> Department of Astronomy, University of Washington, Box 351580, Seattle, WA 98195.

<sup>4</sup> Princeton University Observatory, Peyton Hall, Princeton, NJ 08544-1001.

<sup>5</sup> Department of Physics and Astronomy, Johns Hopkins University, 3400 North Charles Street, Baltimore, MD 21218-2686.

<sup>6</sup> Yerkes Observatory, University of Chicago, 373 West Geneva Street, Williams Bay, WI 53191.

<sup>7</sup> Apache Point Observatory, P.O. Box 59, Sunspot, NM 88349.

<sup>8</sup> Department of Astronomy, 105-24, California Institute of Technology, 1201 East California Boulevard, Pasadena, CA 91125.

<sup>9</sup> Observatoire Midi-Pyrénées, 14 avenue Edouard Belin, F-31400 Toulouse, France.

<sup>10</sup> Department of Physics and Astronomy, University of Pittsburgh, 3941 O'Hara Street, Pittsburgh, PA 15260.

<sup>11</sup> Department of Physics of Complex Systems, Eötvös University, Pázmány Péter sétány 1/A, H-1117 Budapest, Hungary.

<sup>12</sup> Department of Astronomy and Research Center for the Early Universe, School of Science, University of Tokyo, 7-3-1 Hongo, Bunkyo, Tokyo 113-0033, Japan.

<sup>13</sup> Institute for Advanced Study, Olden Lane, Princeton, NJ 08540-0631.

<sup>14</sup> Hubble Fellow.

<sup>15</sup> Department of Physics, Yale University, P.O. Box 208121, New Haven, CT 06520.

<sup>16</sup> National Astronomical Observatory, 2-21-1 Osawa, Mitaka, Tokyo 181-8588, Japan.

<sup>17</sup> Institute for Cosmic Ray Research, University of Tokyo, 3-2-1 Midori, Tanashi, Tokyo 188-8502, Japan.

<sup>18</sup> US Naval Observatory, Flagstaff Station, P.O. Box 1149, Flagstaff, AZ 86002.

<sup>19</sup> US Naval Observatory, 3450 Massachusetts Avenue, NW, Washington, DC 20392-5420.

<sup>20</sup> Remote Sensing Division, Code 7215, Naval Research Laboratory, 4555 Overlook Avenue, SW, Washington, DC 20375.

<sup>21</sup> Observatories of the Carnegie Institution of Washington, 813 Santa Barbara Street, Pasadena, CA 91101.

<sup>22</sup> Astronomical Institute, Tohoku University, Aramaki, Aoba, Sendai 980-8578, Japan.

## 1. INTRODUCTION

At this writing (2000 May), the Sloan Digital Sky Survey (SDSS) is ending its commissioning phase and beginning operations. The purpose of this paper is to provide a concise summary of the vital statistics of the project, a definition of some of the terms used in the survey, and, via links to documentation in electronic form, access to detailed descriptions of the project's design, hardware, and software, to serve as technical background for the project's science papers. The electronic material is extracted from the text (the "Project Book") written to support major funding proposals and is available at the Astronomical Journal World Wide Web site via the on-line version of this paper. The official SDSS Web site also provides links to the on-line Project Book.<sup>37</sup> The versions accessible at the SDSS Web sites also contain extensive discussions and summaries of the scientific goals of the survey, which are not included here.

The text of the on-line Project Book was last updated in 1997 August. While there have been a number of changes in the hardware and software described therein, the material accurately describes the design goals and the implementation of the major observing subsystems. As the project becomes operational, we will provide a series of formal technical papers (most still in preparation) that will describe in detail the project hardware and software in its actual operational state.

Section 2 describes the survey's objectives: the imaging depth, sky coverage, and instrumentation. Section 3 summarizes the software and data reduction components of the SDSS and its data products. Section 4 reviews some recent scientific results from the project's initial commissioning data runs, which demonstrate the ability of the project to reach its technical goals. All celestial coordinates are in equinox J2000.0.

## 2. SURVEY CHARACTERISTICS

The SDSS will produce both imaging and spectroscopic surveys over a large area of the sky. The survey uses a dedicated 2.5 m telescope equipped with a large-format mosaic CCD camera to image the sky in five optical bands, and two digital spectrographs to obtain the spectra of about 1 million galaxies and 100,000 quasars selected from the imaging data.

The SDSS calibrates its photometry using observations of a network of standard stars established by the US Naval Observatory (USNO) 1 m telescope, and its astrometry is calibrated using observations by an array of astrometric CCDs in the imaging camera.

### 2.1. Telescope

The SDSS telescope is a 2.5 m f/5 modified Ritchey-Chrétien wide-field altitude-azimuth telescope (see Project Book § 2, "The Telescope") located at the Apache Point Observatory (APO), Sunspot, New Mexico (§ 3, "The Site"). The telescope achieves a very wide ( $3^{\circ}$ ) distortion-free field by the use of a large secondary mirror and two corrector lenses. It is equipped with the photometric/astrometric mosaic camera (§ 4, "The Photometric Camera"; Gunn et al. 1998) and images the sky by scanning along great circles at the sidereal rate. The imaging camera mounts at the Cassegrain focus. The telescope is also equipped with two double fiber-fed spectrographs, permanently mounted on the image rotator, since the spectrographs are fiber fed. This ensures that the fibers do not flex during an exposure. The telescope is changed from imaging mode to spectroscopic mode by removing the imaging camera and mounting at the Cassegrain focus a fiber plug plate, individually drilled for each field, which feeds the spectrographs. In survey operations, it is expected that up to nine spectroscopic plates per night will be observed, with the necessary plates being plugged with fibers during the day. The telescope mounting and enclosure allow easy access for rapid changes between fiber plug plates and between spectroscopic and imaging modes. This strategy allows imaging to be done in pristine observing conditions (photometric sky, image size  $\leq 1.5''$  FWHM) and spectroscopy to be done during less ideal conditions. All observing will be done in moonless sky.

Besides the 2.5 m telescope, the SDSS makes use of three subsidiary instruments at the site. The *photometric telescope* (PT) is a 0.5 m telescope equipped with a CCD camera and the SDSS filter set. Its task is to calibrate the photometry. Two instruments, a *seeing monitor* and a  $10 \mu\text{m}$  *cloud scanner* (Hull, Limmongkol, & Siegmund 1994; Project Book § 3), monitor the astronomical weather.

### 2.2. Imaging Camera

The SDSS imaging camera contains two sets of CCD arrays: the *imaging array* and the *astrometric arrays* (Project Book § 4; Gunn et al. 1998). The *imaging array* consists of 30  $2048 \times 2048$  Tektronix CCDs, placed in an array of six columns and five rows. The telescope's scanning is aligned with the columns. Each row observes the sky through a different filter, in temporal sequence  $r'$ ,  $i'$ ,  $u'$ ,  $z'$ , and  $g'$ . The pixel size is  $24 \mu\text{m}$  ( $0.396''$  on the sky). The imaging survey is taken in drift-scan (time-delay and integrate, or TDI) mode, i.e., the camera continually sweeps the sky in great circles, and a given point on the sky passes

<sup>23</sup> Merrill Lynch Japan Incorporated, 1-1-3 Otemachi, Chiyoda, Tokyo 100, Japan.

<sup>24</sup> Los Alamos National Laboratory, P.O. Box 1663, Los Alamos, NM 87545.

<sup>25</sup> Department of Physics, University of Michigan, 500 East University, Ann Arbor, MI 48109-1120.

<sup>26</sup> Royal Observatory, Edinburgh, Blackford Hill, Edinburgh EH9 3JH, UK.

<sup>27</sup> Department of Physics, Carnegie Mellon University, 5000 Forbes Avenue, Pittsburgh, PA 15232.

<sup>28</sup> Department of Physics, Applied Physics, and Astronomy, Rensselaer Polytechnic Institute, 110 Eighth Street, Troy, NY 12180-3590.

<sup>29</sup> Lucent Technologies, 2000 North Naperville Road, Naperville, IL 60566.

<sup>30</sup> Divisione di Astronomia e Astrofisica, Osservatorio Astronomico di Trieste, via G. B. Tiepolo 11, I-34131 Trieste, Italy.

<sup>31</sup> Department of Physics, Rochester Institute of Technology, 85 Lomb Memorial Drive, Rochester, NY 14623-5603.

<sup>32</sup> Department of Astronomy and Astrophysics, 525 Davey Laboratory, Pennsylvania State University, University Park, PA 16802.

<sup>33</sup> Canadian Institute for Theoretical Astrophysics, University of Toronto, 60 St. George Street, Toronto, ON M5S 3H8, Canada.

<sup>34</sup> Department of Physics, Drexel University, 3141 Chestnut Street, Philadelphia, PA 19104.

<sup>35</sup> Institute of Space and Astronautical Science, 3-1-1 Yoshinodai, Sagamihara, Kanagawa 229, Japan.

<sup>36</sup> Department of Astronomy, Ohio State University, 140 West 18th Avenue, Columbus, OH 43210-1173.

<sup>37</sup> It can also be accessed directly at <http://www.astro.princeton.edu/PBOOK/welcome.htm>.

through the five filters in succession. The effective integration time per filter is 54.1 s, and the time for passage over the entire photometric array is about 5.7 minutes (Project Book § 1, "Survey Strategy"; Gunn et al. 1998). Since the camera contains six columns of CCDs, the result is a long *strip* of six *scan lines*, containing almost simultaneously observed five-color data for each of the six CCD columns. Each CCD observes a swath of sky 13'.52 wide. The CCDs are separated in the *row* direction (i.e., perpendicular to the scan direction) by 91.0 mm (25'2 on the sky) center to center. The observations are filled in by a second strip, offset from the first by 93% of the CCD width, to produce a filled *stripe*, 2'.54 wide, with 8% (1') lateral overlap on each side. Because of the camera's large field of view, the TDI tracking must be done along great circles. The northern Galactic cap is covered by 45 great-circle arcs (shown projected on the sky in Figs. 1 and 2).

### 2.3. Photometry and Photometric Calibration

The five filters in the imaging array of the camera,  $u'$ ,  $g'$ ,  $r'$ ,  $i'$ , and  $z'$ , have design effective wavelengths of 3550, 4770, 6230, 7620, and 9130 Å, respectively (Fukugita et al. 1996; Gunn et al. 1998). The close-to-final values are 3560, 4680, 6180, 7500, and 8870 Å. An a priori model estimate of the telescope and camera throughputs and of the sky brightness predicted that we would reach the  $5\sigma$  detection limit for point sources in 1" seeing at 22.3, 23.3, 23.1, 22.3, and 20.8 in the  $u'$ ,  $g'$ ,  $r'$ ,  $i'$ , and  $z'$  filters, respectively, at an air mass of 1.4. We have put formal requirements on throughput at 75% of the values used for the above estimation and have demonstrated that we meet this requirement in all bands with the possible exception of  $z'$ . The sensitivity limit can be tested by finding the magnitude at which repeat observations of a given area of sky yield 50% reproducibility of the objects detected. This has been tested most thoroughly with data taken in less than optimal seeing (1''.3–1''.6); nevertheless, the 50% reproducibility level lies within a few tenths of a magnitude of the above-quoted  $5\sigma$  detection limit in all five bands (see Ivezić et al. 2000). The SDSS science requirements demand that photometric calibration uncertainties for point sources be 0.02 in  $r'$ , 0.02 in  $r'-i'$  and  $g'-r'$ , and 0.03 in  $u'-g'$  and  $i'-z'$ . To meet these stringent requirements in both signal-to-noise ratio and photometricity, imaging data are declared to be of survey quality only if the PT determines that the night is photometric, with a zero-point uncertainty below 1%, and if the seeing is better than 1''.5. The imaging data saturate at about 13, 14, 14, 14, and 12 mag for point sources.

The magnitude scale is on the AB<sub>v</sub> system (J. B. Oke 1969, unpublished), which was updated to the AB<sub>79</sub> system by Oke & Gunn (1983) and to AB<sub>95</sub> by Fukugita et al. (1996). The magnitudes  $m$  are related to flux density  $f$  by  $m \sim \sinh^{-1} f$  rather than logarithmically (see Lupton, Gunn, & Szalay 1999; Fan et al. 1999c). This definition is essentially identical to the logarithmic magnitude at signal-to-noise ratios greater than about 5 and is well behaved for low and even zero and negative flux densities.

The calibration and definition of the magnitude system are carried out by the USNO 1 m telescope and the 0.5 m PT. The SDSS photometry is placed on the AB<sub>v</sub> system using three *fundamental standards* (BD +17°4708, +26°2606, and +21°609), whose magnitude scale is as defined by Fukugita et al. (1996); a set of 157 *primary standards*, which are calibrated by the above fundamental stan-

dards using the USNO 1 m telescope, and which cover the whole range of right ascension and enable the calibration system to be made self-consistent; and a set of *secondary calibration patches* lying across the imaging stripes, containing stars fainter than 14 mag whose magnitudes are calibrated by the PT with respect to those of the primary standards and which transfer that calibration to the imaging survey. The locations of these patches on the survey stripes are shown in Figure 1. On nights when the 2.5 m is observing, the PT observes primary standard stars to provide the atmospheric extinction coefficients over the night and to confirm that the night is photometric. The standard star network is described in Project Book § 5, "Photometric Calibration"—note that the telescope described there has now been replaced by the 0.5 m PT.

### 2.4. Astrometric Calibration

The camera also contains leading and trailing *astrometric arrays*: narrow ( $128 \times 2048$ ), neutral-density-filtered,  $r'$ -filtered CCDs covering the entire width of the camera. These arrays can measure objects in the magnitude range  $r' \sim 8.5$ –16.8, i.e., they cover the dynamic range between the standard astrometric catalog stars and the brightest unsaturated stars in the photometric array. The astrometric calibration is thereby referenced to the fundamental astrometric catalogs (see Project Book § 6, "Astrometry"), using the Hipparcos and Tycho Catalogues (ESA 1997) and specially observed equatorial fields (Stone, Pier, & Monet 1999). Comparison with positions from the FIRST (Becker, White, & Helfand 1995) and 2MASS (Skrutskie 1999) catalogs shows that the rms astrometric accuracy is currently better than 150 mas in each coordinate.

### 2.5. Imaging Survey: North Galactic Cap

The imaging survey covers about 10,000 contiguous square degrees in the northern Galactic cap. This area lies

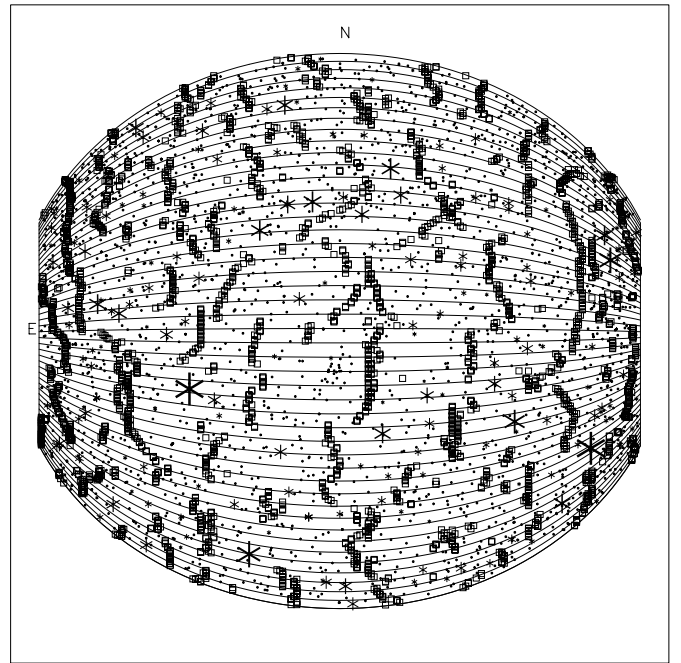


FIG. 1.—Projection on the sky of the northern SDSS survey area. The positions of the Yale Bright Star Catalogue stars are shown. The largest symbols are stars of 0 mag, and the smallest, stars of 5–7 mag. The secondary calibration patches are shown by squares.

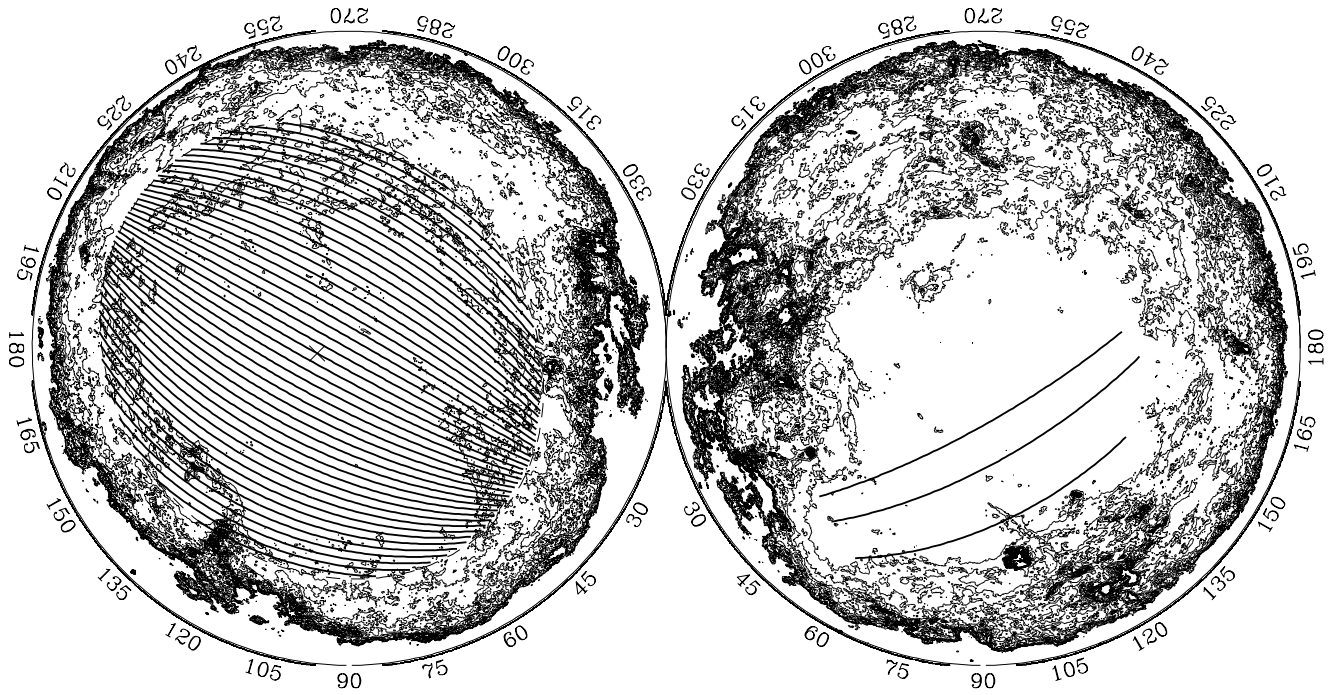


FIG. 2.—Projection on the sky (Galactic coordinates) of the northern (left) and southern (right) SDSS surveys. The lines show the individual stripes to be scanned by the imaging camera. These are overlaid on the extinction contours of Schlegel, Finkbeiner, & Davis (1998). The survey pole is marked by the cross.

basically above Galactic latitude  $30^\circ$ , but its footprint is adjusted slightly to lie within the minimum of the Galactic extinction contours (Schlegel, Finkbeiner, & Davis 1998), resulting in an elliptical region. The region is centered at  $\alpha = 12^{\text{h}}20^{\text{m}}$ ,  $\delta = +32.5^\circ$ . The minor axis is at an angle  $20^\circ$  east of north with extent  $\pm 55^\circ$ . The major axis is a great circle perpendicular to the minor axis with extent  $\pm 65^\circ$ . The survey footprint with the location of the stripes is shown in Figure 2—see Project Book § 1 for details.

### 2.6. Imaging Survey: The South Galactic Cap

In the south Galactic cap, three stripes will be observed, one along the celestial equator and the other two north and south of the equator (see Fig. 2). The *equatorial stripe* ( $\alpha = 20^{\text{h}}7$  to  $4^{\text{h}}$ ,  $\delta = 0^\circ$ ) will be observed repeatedly, both to find variable objects and, when co-added, to reach magnitude limits about 2 mag deeper than the northern imaging survey. The other two stripes will cover great circles lying between right ascension and declination of  $(20^{\text{h}}7, -5^\circ8)$  to  $(4^{\text{h}}0, -5^\circ8)$  and  $(22^{\text{h}}4, 8^\circ7)$  to  $(2^{\text{h}}3, 13^\circ2)$ .

### 2.7. Spectroscopic Survey

Objects are detected in the imaging survey, classified as point source or extended, and measured, by the image analysis software (see below). These imaging data are used to select in a uniform way different classes of objects whose spectra will be taken. The final details of this *target selection* will be described once the survey is well underway; the criteria discussed here are likely to be very close to those finally used.

Two samples of galaxies are selected from the objects classified as “extended.” About  $9 \times 10^5$  galaxies will be selected to have Petrosian (1976) magnitudes  $r'_P \leq 17.7$ . Galaxies with a mean  $r'$ -band surface brightness within the half-light radius fainter than 24 mag  $\text{arcsec}^{-2}$  will be

removed, since spectroscopic observations are unlikely to produce a redshift. For illustrative purposes, a simulation of a slice of the SDSS redshift survey is shown in Figure 3 (from Colley et al. 2000). Galaxies in this cold dark matter simulation are “selected” by the SDSS selection criteria. As Figure 3 demonstrates, the SDSS volume is large enough to contain a statistically significant sample of the largest structures predicted.

The second sample, of approximately  $10^5$  galaxies, exploits the characteristic very red color and high metallicity (producing strong absorption lines) of the most luminous galaxies: the “brightest cluster galaxies” or “bright red galaxies” (BRGs); redshifts can be well measured with the SDSS spectra for these galaxies to about  $r' = 19.5$ . Galaxies located at the dynamical centers of nearby dense clusters often have these properties. Reasonably accurate photometric redshifts (Connolly et al. 1995) can be determined for these galaxies, allowing the selection by magnitude and  $g'r'i'$  color of an essentially *distance-limited* sample

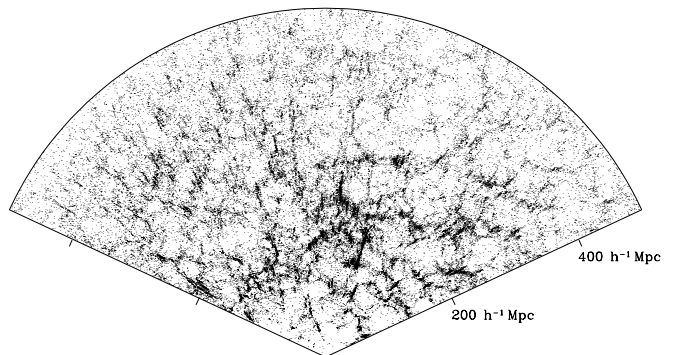


FIG. 3.—A 6°-wide slice of the simulated SDSS (from Colley et al. 2000), showing about 1/20 of the survey.

of the highest density regions of the universe to a redshift of about 0.45 (see Fig. 4 for a simulation).

With their power-law continua and the influence of Ly $\alpha$  emission and the Ly $\alpha$  forest, quasars have  $u'g'r'i'z'$  colors quite distinct from those of the vastly more numerous stars over most of their redshift range (Fan 1999). Thus, about  $1.5 \times 10^5$  quasar candidates are selected for spectroscopic observations as outliers from the stellar locus (cf. Krisciunas, Margon, & Szkody 1998; Lenz et al. 1998; Newberg et al. 1999; Fig. 5 below) in color-color space. At the cost of some loss of efficiency, selection is allowed closer to the stellar locus around  $z = 2.8$ , where quasar colors approach those of early F and late A stars (Newberg & Yanny 1997; Fan 1999). Some further regions of color-color space outside the main part of the stellar locus where quasars are very rarely found are also excluded, including the regions containing M dwarf-white dwarf pairs, early A stars, and white dwarfs (see Fig. 5). The SDSS will compile a sample of quasars brighter than  $i' \approx 19$  at  $z < 3.0$ ; at redshifts between 3.0 and about 5.2, the limiting magnitude will be about  $i' = 20$ . Objects are also required to be point sources, except in the region of color-color space where low-redshift quasars are expected to be found. Stellar objects brighter than  $i' = 20$  that are FIRST sources (Becker et al. 1995) are also selected. Based on early spectroscopy, we estimate that

roughly 65% of our quasar candidates are genuine quasars; comparison with samples of known quasars indicates that our completeness is of order 90%.

In all cases, the magnitudes of the objects are corrected for Galactic extinction before selection, using extinction in the SDSS bands calculated from the reddening map of Schlegel et al. (1998). Objects are then selected to have a magnitude limit *outside* the Galaxy. If this correction were not made, the systematic effects of Galactic extinction over the survey area would overwhelm the statistical uncertainties in the SDSS data set. After the imaging and spectroscopic survey is completed in a given part of the sky, the reddening and extinction will be recalculated using internal standards extracted from the imaging data. We plan to use a variety of extinction probes, including very hot halo subdwarfs, halo turnoff stars, and elliptical galaxies whose intrinsic colors can be estimated from their line indices.

Together with various classes of calibration stars and fibers that observe blank sky to measure the sky spectrum, the selected galaxies and quasars are mapped onto the sky and “tiled,” i.e., their location on a  $3^\circ$  diameter plug plate determined (Project Book § 8, “Adaptive Tiling”). The centers of the tiles are adjusted to provide closer coverage of regions of high galactic surface density, to make the spectro-

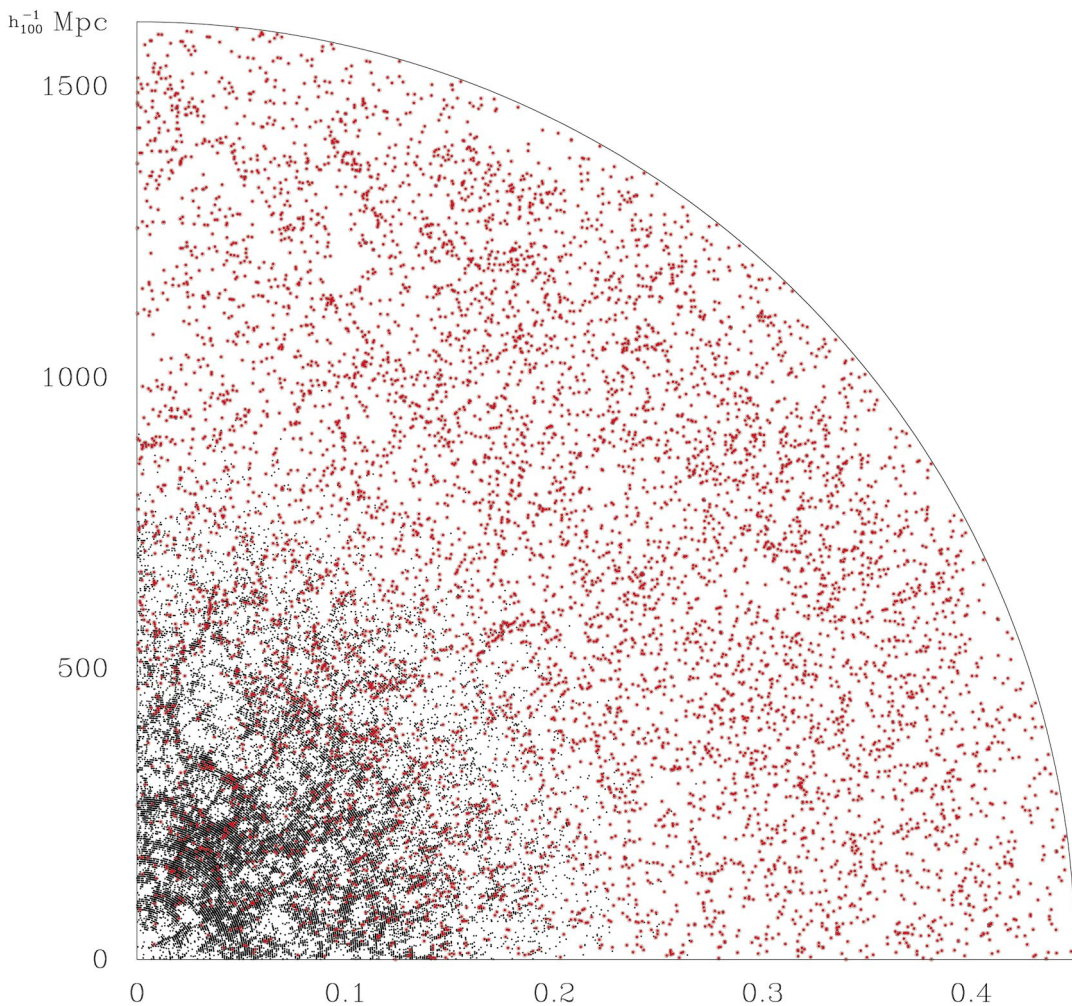


FIG. 4.—Simulated redshift distribution in a  $6^\circ$  slice of the SDSS. Small dots, main galaxy sample (cf. Fig. 3); large red dots, the BRG sample, showing about 1/30 of the survey.

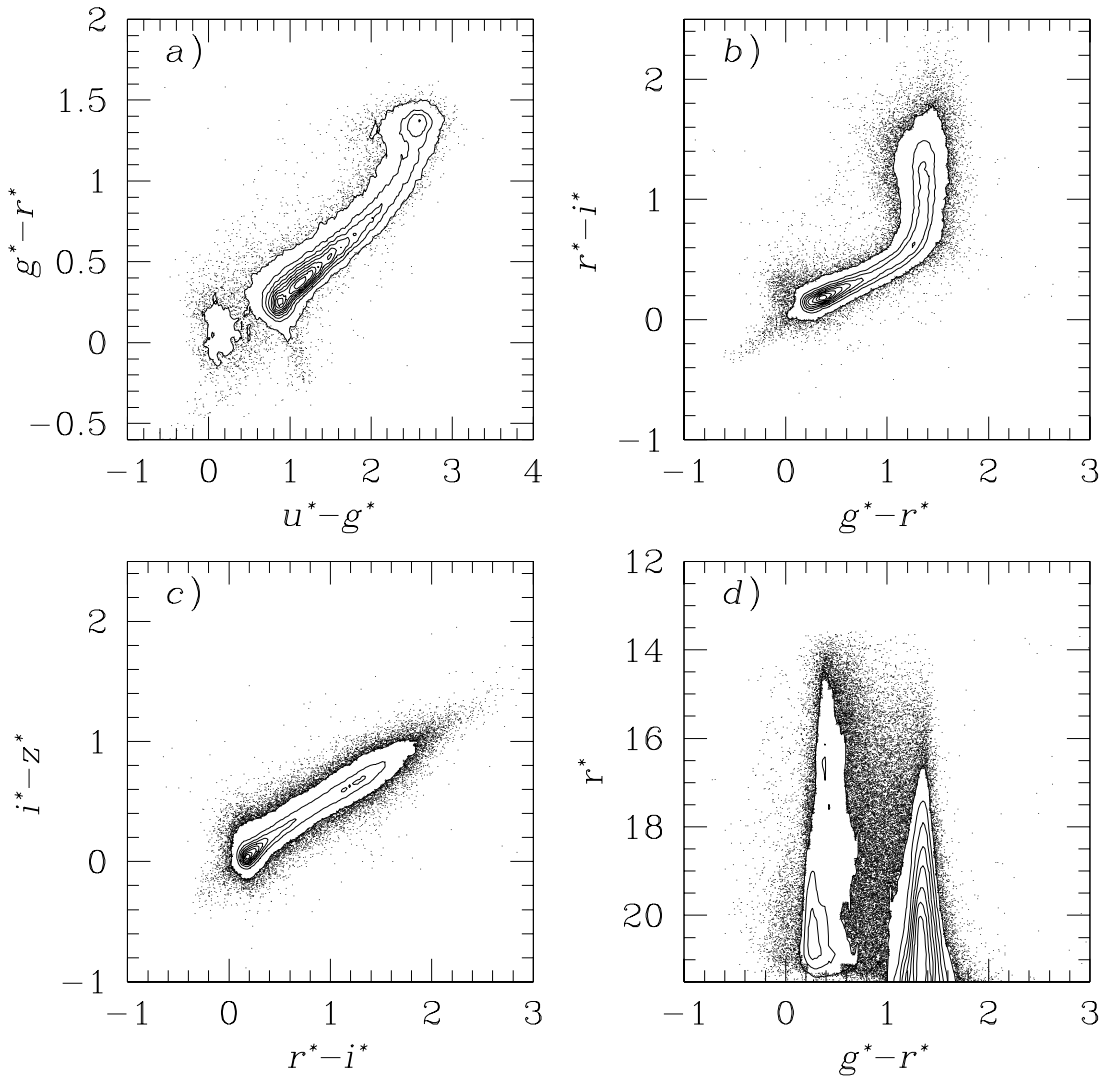


FIG. 5.—Color-color and color-magnitude plots of about 117,000 point sources brighter than 21 mag at  $i^*$  and detected at greater than  $5\sigma$  in each band from  $25 \text{ deg}^2$  of SDSS imaging data, reduced by the photometric pipeline (the  $i^*$  designation is used for preliminary SDSS photometry). The contours are drawn at intervals of 10% of the peak density of points. The redder stars extend to fainter magnitudes than do the bluer stars, because of the  $i^*$  limit.

scopic coverage optimally uniform. Excess fibers are allocated to several classes of rare or peculiar objects (e.g., objects that are positionally matched with *ROSAT* sources, or those whose parameters lie outside any known range—these are *serendipitous* objects) and to samples of stars. The spectra are observed, 640 at a time (with a total integration time of 45–60 minutes depending on observing conditions) using a pair of fiber-fed double spectrographs (§ 7, “Spectroscopy”). The wavelength coverage of the spectrographs is continuous from about 3800 to 9200 Å, and the wavelength resolution,  $\lambda/\delta\lambda$ , is 1800 (Uomoto et al. 1999). The fibers are located at the focal plane via plug plates constructed for each area of sky. The fiber diameter is 0.2 mm (3" on the sky), and adjacent fibers cannot be located more closely than 55" on the sky. Both members of a pair of objects closer than this separation can be observed spectroscopically if they are located in the overlapping regions of adjacent tiles.

Tests of the redshift accuracy using observations of stars in M67 whose radial velocities are accurately known (Mathieu et al. 1986) show that the SDSS radial velocity measurements for stars have a scatter of about  $3.5 \text{ km s}^{-1}$ .

### 3. SOFTWARE AND DATA PRODUCTS

The operational software is described in Project Book § 10, “Datasystems.” The data are obtained using the data acquisition system at APO (Petravick et al. 1994) and recorded on digital linear tape. The imaging data consist of full images from all CCDs of the imaging array, cutouts of detected objects from the astrometric array, and bookkeeping information. These tapes are shipped to Fermilab by express courier, and the data are automatically reduced through an interoperating set of software pipelines operating in a common computing environment.

The *photometric pipeline* reduces the imaging data; it corrects the data for data defects (interpolation over bad columns and bleed trails, finding and interpolating over “cosmic rays,” etc.), calculates overscan (bias), sky, and flat-field values, calculates the point-spread functions (PSFs) as a function of time and location on the CCD array, finds objects, combines the data from the five bands, carries out simple model fits to the images of each object, deblends overlapping objects, and measures positions, magnitudes (including PSF and Petrosian magnitudes), and shape

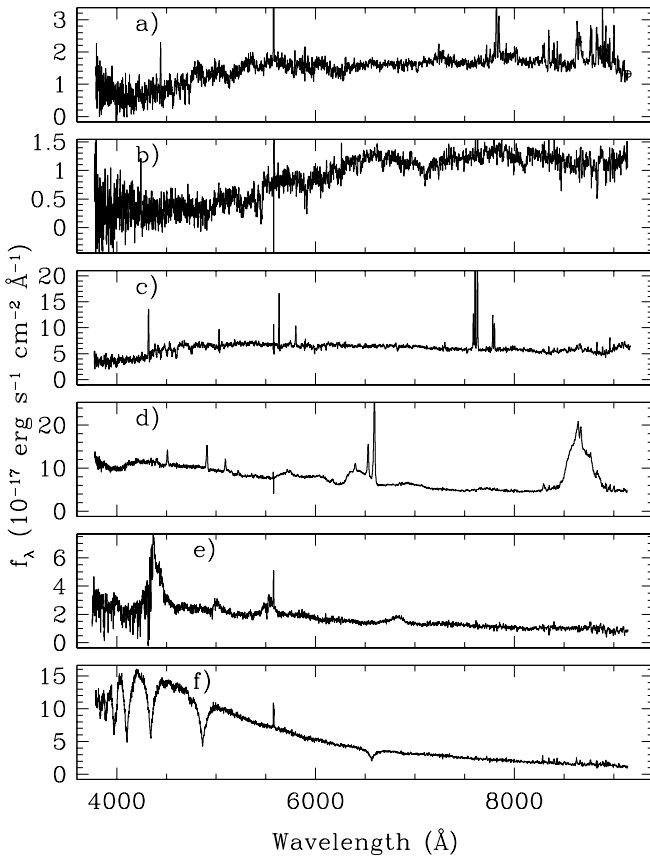


FIG. 6.—Representative SDSS spectra taken from a single spectroscopic plate observed on 1999 October 4 for a total of 1 hr of integration time, processed by the SDSS spectroscopic pipeline. For display purposes, all spectra have been smoothed with a 3 pixel boxcar function. All spectra show significant residuals due to the strong sky line at 5577 Å. The objects depicted are as follows: (a) An  $r_p^* = 18.00$  galaxy;  $z = 0.1913$ . This object is slightly fainter than the main galaxy target selection limit. Note the H $\alpha$ /[N II] emission at  $\sim 7800$  Å, [O II] emission at  $\sim 4450$  Å, and Ca II H and K absorption at  $\sim 4700$  Å. (b) An  $r_p^* = 19.41$  galaxy;  $z = 0.3735$ . This object is close to the photometric limit of the BRG sample. The H and K lines are particularly strong. (c) A star-forming galaxy with  $r_p^* = 16.88$ , at  $z = 0.1582$ . (d) A  $z = 0.3162$  quasar, with  $r_{\text{psf}}^* = 16.67$ . Note the unusual profile shape of the Balmer lines. This quasar is LBQS 0004 + 0036 (Morris et al. 1991). (e) A  $z = 2.575$  quasar with  $r_{\text{psf}}^* = 19.04$ ; note the resolution of the Ly $\alpha$  forest. This quasar was discovered by Berger & Fringant (1985). (f) A hot white dwarf, with  $r_{\text{psf}}^* = 18.09$ .

parameters. The photometric pipeline uses position calibration information from the astrometric array reduced through the *astrometric pipeline* and photometric calibration data from the photometric telescope (reduced through the *photometric telescope pipeline*). Final calibrations are applied by the *final calibration pipeline*, which allows refinements in the positional and photometric calibration as the survey progresses. The photometric pipeline is extensively tested using repeat observations, examination of the outputs, observations of regions of the sky previously observed by other telescopes (*Hubble Space Telescope* fields, for example), and a set of simulations, described in detail in Project Book § 9, “Simulations.” For an example of the repeatability of SDSS photometry over several timescales, see Ivezić et al. (2000). These repeat observations show that the mean errors (for point sources) are about 0.03 mag to 20 mag, increasing to about 0.05 mag at 21 mag and to 0.12 mag at 22 mag. These observed errors are in good agreement with those quoted by the photometric pipeline. They

apply only to the  $g'$ ,  $r'$ , and  $i'$  bands—in the less sensitive  $u'$  and  $z'$  bands, the errors at the bright end are about the same as those in  $g'r'i'$  but increase to 0.05 at 20 mag and 0.12 at 21 mag.

The outputs, together with all the observing and processing information, are loaded into the *operational database*, which is the central collection of scientific and bookkeeping data used to run the survey. To select the spectroscopic targets, objects are run through the *target selection pipeline* and flagged if they meet the spectroscopic selection criteria for a particular type of object. The criteria for the primary objects (quasars, galaxies, and BRGs) will not be changed once the survey is underway. Those for serendipitous objects and samples of interesting stars can be changed throughout the survey. A given object can in principle receive several target flags. The selected objects are tiled as described above, plug plates are drilled, and the spectroscopic observations are made. The spectroscopic data are automatically reduced by the *spectroscopic pipeline*, which extracts, corrects, and calibrates the spectra, determines the spectral types, and measures the redshifts. The reduced spectra are then stored in the operational database. The contents of the operational database are copied at regular intervals into the *science database* for retrieval and scientific analysis (see Project Book § 11, “The Science Archive”). The science database is indexed in a hierarchical manner: the data and other information are linked into “containers” that can be divided and subdivided as necessary, to define easily searchable regions with approximately the same data content. This hierarchical scheme is consistent with those being adopted by other large surveys, to allow cross-referencing of multiple surveys. The science database also incorporates a set of query tools and is designed for easy portability.

The photometric data products of the SDSS include a *catalog* of all detected objects, with measured positions, magnitudes, shape parameters, model fits, and processing flags; *atlas images* (i.e., cutouts from the imaging data in all five bands) of all detected objects and of objects from the FIRST and ROSAT catalogs; a  $4 \times 4$  binned image of the corrected images with the objects removed; and a *mask* of the areas of sky not processed (because of saturated stars, for example) and of corrected pixels (e.g., those from which cosmic rays were removed). The atlas images are sized to enclose the area occupied by each object plus the PSF width, or the object size given in the ROSAT or FIRST catalog.<sup>38</sup> The database will also contain the calibrated one-dimensional *spectra*, the derived *redshift* and *spectral type*, and the bookkeeping information related to the spectroscopic observations. In addition, the positions of astrometric calibration stars measured by the astrometric pipeline and the magnitudes of the faint photometric standards measured by the photometric telescope pipeline will be published at regular intervals.

#### 4. EARLY SCIENCE FROM THE SDSS COMMISSIONING DATA

The goal of the SDSS is to provide the data necessary for studies of the large-scale structure of the universe on a wide range of scales. The imaging survey should detect  $\sim 5 \times 10^7$

<sup>38</sup> The photometric outputs are described at <http://www.astro.princeton.edu/SDSS/photo.html>.



FIG. 7.—Sample frame ( $13' \times 9'$ ) from the SDSS imaging commissioning data. The image, a color composite made from the  $g'$ ,  $r'$ , and  $i'$  data, shows a field containing the distant cluster Abell 267 ( $\alpha = 01^{\text{h}}52^{\text{m}}41^{\text{s}}0$ ,  $\delta = +01^{\circ}00'24\overset{''}{.}7$ , redshift  $z = 0.23$ ; Crawford et al. 1999); this is the cluster of galaxies with yellow colors in the lower center of the frame. The frame also contains, in the upper center, the nearby cluster RX J0153.2+0102, estimated redshift  $\sim 0.07$  (Bade et al. 1998) ( $\alpha = 01^{\text{h}}53^{\text{m}}15\overset{\text{s}}{.}15$ ,  $\delta = +01^{\circ}02'18\overset{''}{.}8$ ). The PSF (optics plus seeing) was about  $1\overset{''}{.}6$ . Right ascension increases from bottom to top of the frame, declination from left to right.

galaxies,  $\sim 10^6$  quasars, and  $\sim 8 \times 10^7$  stars to the survey limits. These photometric data, via photometric redshifts and various statistical techniques such as the angular correlation function, support studies of large-scale structure well past the limit of the spectroscopic survey. On even larger scales, information on structure will come from quasars.

The science justification for the SDSS is discussed in several conference papers (e.g., Gunn & Weinberg 1995; Fukugita 1998; Margon 1999).<sup>39</sup> Much of the science for which the SDSS was built, the study of large-scale structure, will come when the survey is complete, but the initial test data have already led to significant scientific discoveries in many fields. In this section, we show examples of the first test data and some initial results. To date (2000 May), the SDSS has obtained test imaging data for some  $2000 \text{ deg}^2$  of sky and about 20,000 spectra. Examples of these data are shown in Figure 5 (sample color-color and color-magnitude

diagrams of point-source objects), Figure 6 (sample spectra), and Figure 7 (a composite color image of a piece of the sky that contains the cluster Abell 267).

Fischer et al. (2000) have detected the signature of the weak lensing of background galaxies by foreground galaxies, allowing the halos and total masses of the foreground galaxies to be measured. The searches by Fan et al. (1999a, 1999c, 2000b, 2000c), Schneider et al. (2000), and Zheng et al. (2000) have greatly increased the number of known high-redshift ( $z > 3.6$ ) quasars and include several quasars with  $z > 5$ . Fan et al. (1999a) have found the first example of a new kind of quasar: a high-redshift object with a featureless spectrum and without the radio emission and polarization characteristics of BL Lacertae objects. The redshift for this object ( $z = 4.6$ ) was found from the Ly $\alpha$  forest absorption in the spectrum.

Some 150 distant probable RR Lyrae stars have been found in the Galactic halo, enabling the halo stellar density to be mapped; the distribution may have located the edge of the halo at approximately 60 kpc (Ivezić et al. 2000). The distribution of RR Lyrae stars and other horizontal-branch

<sup>39</sup> The Project Book science sections can be accessed at <http://www.astro.princeton.edu/PBOOK/science/science.htm>.

stars is very clumped, showing the presence of possible tidal streamers in the halo (Ivezić et al. 2000; Yanny et al. 2000). Margon et al. (1999) describe the discovery of faint high-latitude carbon stars in the SDSS data.

Strauss et al. (1999), Schneider et al. (2000), Fan et al. (2000a), Tsvetanov et al. (2000), Pier et al. (2000), and Leggett et al. (2000) report the discovery of a number of very low mass stars or substellar objects, those of type "L" or "T," including the first field methane ("T") dwarfs and the first stars of spectral type intermediate between L and T. The detection rate to date shows that the SDSS is likely to identify several thousand L and T dwarfs. These objects are found to occupy very distinct regions of color-color and color-magnitude space, which will enable the completeness of the samples to be well characterized.

Measurements of the PSF diameter variations and the image wander allow variations in the turbulence in Earth's atmosphere to be tracked. These data demonstrate the presence of anomalous refraction on scales at least as large as the 2°3 field of view of the camera (Pier et al. 1999).

Of course, the most exciting possibility for any large survey that probes new regions of sensitivity or wavelength

is the discovery of exceedingly rare or entirely new classes of objects. The SDSS has already found a number of very unusual objects; the nature of some of these remains unknown (Fan et al. 1999b). These and other investigations in progress show the promise of SDSS for greatly advancing astronomical work in fields ranging from the behavior of Earth's atmosphere to structure on the scale of the horizon of the universe.

The Sloan Digital Sky Survey is a joint project of the University of Chicago, Fermilab, the Institute for Advanced Study, the Japan Participation Group, Johns Hopkins University, the Max-Planck-Institut für Astronomie, Princeton University, the US Naval Observatory, and the University of Washington. Apache Point Observatory, site of the SDSS, is operated by the Astrophysical Research Consortium. Funding for the project has been provided by the Alfred P. Sloan Foundation, the SDSS member institutions, the National Aeronautics and Space Administration, the National Science Foundation, the US Department of Energy, and Monbusho. The official SDSS Web site is [www.sdss.org](http://www.sdss.org).

#### REFERENCES

- Bade, N., et al. 1998, *A&AS*, 127, 145  
 Becker, R. H., White, R. L., & Helfand, D. J. 1995, *ApJ*, 450, 559  
 Berger, J., & Fringant, A.-M. 1985, *A&AS*, 61, 191  
 Colley, W. N., Gott, J. R., III, Weinberg, D. H., Park, C., & Berlind, A. A. 2000, *ApJ*, 529, 795  
 Connolly, A. J., Čsabai, I., Szalay, A. S., Koo, D. C., Kron, R. G., & Munn, J. A. 1995, *AJ*, 110, 2655  
 Crawford, C. S., Allen, S. W., Ebeling, H., Edge, A. C., & Fabian, A. C. 1999, *MNRAS*, 306, 857  
 ESA. 1997, The Hipparcos and Tycho Catalogues (ESA SP-1200) (Noordwijk: ESA)  
 Fan, X. 1999, *AJ*, 117, 2528  
 Fan, X., et al. 2000a, *AJ*, 119, 928  
 —. 1999a, *ApJ*, 526, L57  
 Fan, X., Strauss, M. A., Schneider, D. P., Gunn, J. E., Lupton, R. H., Knapp, G. R., & Yanny, B. 1999b, *BAAS*, 194, No. 73.15  
 Fan, X., et al. 2000b, *AJ*, 119, 1  
 —. 1999c, *AJ*, 118, 1  
 —. 2000c, *AJ*, 120, 1167  
 Fischer, P., et al. 2000, *AJ*, 120, 1198  
 Fukugita, M. 1998, *Highlights Astron.*, 11, 449  
 Fukugita, M., Ichikawa, T., Gunn, J. E., Doi, M., Shimasaku, K., & Schneider, D. P. 1996, *AJ*, 111, 1748  
 Gunn, J. E., Carr, M. A., Rockosi, C. M., Sekiguchi, M., et al. 1998, *AJ*, 116, 3040  
 Gunn, J. E., & Weinberg, D. H. 1995, in *Wide Field Spectroscopy and the Distant Universe*, ed. S. Maddox & A. Aragón-Salamanca (Singapore: World Sci.), 3  
 Hull, C. L., Limmongkol, S., & Siegmund, W. A. 1994, *Proc. SPIE*, 2199, 852  
 Ivezić, Ž., et al. 2000, *AJ*, 120, 963  
 Krisciunas, K., Margon, B., & Szkody, P. 1998, *PASP*, 110, 1342  
 Leggett, S. K., et al. 2000, *ApJ*, 536, L35  
 Lenz, D. D., Newberg, H. J., Rosner, R., Richards, G. T., & Stoughton, C. 1998, *ApJS*, 119, 121  
 Lupton, R. H., Gunn, J. E., & Szalay, A. S. 1999, *AJ*, 118, 1406  
 Mathieu, R. D., Latham, D. W., Griffin, R. F., & Gunn, J. E. 1986, *AJ*, 92, 1100  
 Margon, B. 1999, *Phil. Trans. R. Soc. London A*, 357, 93  
 Margon, B., Anderson, S. F., Deutsch, E. W., & Harris, H. C. 1999, *BAAS*, 195, No. 80.06  
 Morris, S. L., Weymann, R. J., Anderson, S. F., Hewett, P. C., Foltz, C. B., Chaffee, F. H., Francis, P. J., & MacAlpine, G. M. 1991, *AJ*, 102, 1627  
 Newberg, H. J., Richards, G. T., Richmond, M., & Fan, X. 1999, *ApJS*, 123, 377  
 Newberg, H. J., & Yanny, B. 1997, *ApJS*, 113, 89  
 Oke, J. B., & Gunn, J. E. 1983, *ApJ*, 266, 713  
 Petravick, D., et al. 1994, *Proc. SPIE*, 2198, 935  
 Petrosian, V. 1976, *ApJ*, 209, L1  
 Pier, J. R., Leggett, S. K., Strauss, M. A., Fan, X., Gunn, J. E., Geballe, T. R., Lupton, R. H., & Knapp, G. R. 2000, in *ASP Conf. Ser.* 212, *From Giant Planets to Cool Stars*, ed. C. A. Griffith & M. S. Marley (San Francisco: ASP), in press  
 Pier, J. R., Munn, J. A., Hennessy, G. S., Hindsley, R. H., & Kent, S. M. 1999, *BAAS*, 195, No. 81.04  
 Schlegel, D. J., Finkbeiner, D. P., & Davis, M. 1998, *ApJ*, 500, 525  
 Schneider, D. P., et al. 2000, *PASP*, 112, 6  
 Skrutskie, M. F. 1999, *BAAS*, 195, No. 34.01  
 Strauss, M. A., et al. 1999, *ApJ*, 522, L61  
 Stone, R. C., Pier, J. R., & Monet, D. G. 1999, *AJ*, 118, 2488  
 Tsvetanov, Z. I., et al. 2000, *ApJ*, 531, L61  
 Uomoto, A., et al. 1999, *BAAS*, 195, No. 87.01  
 Yanny, B., et al. 2000, *ApJ*, 540, 825  
 Zheng, W., et al. 2000, *AJ*, in press